

Chalmers Publication Library



Copyright Notice

©1998 IEEE. Personal use of this material is permitted. However, permission to reprint/republish this material for advertising or promotional purposes or for creating new collective works for resale or redistribution to servers or lists, or to reuse any copyrighted component of this work in other works must be obtained from the IEEE.

(Article begins on next page)

Effects of Self-Heating on Planar Heterostructure Barrier Varactor Diodes

Jan Stake, *Student Member, IEEE*, Lars Dillner, Stephen H. Jones, *Member, IEEE*, Chris Mann, John Thornton, J. Robert Jones, *Member, IEEE*, William L. Bishop, *Member, IEEE*, and Erik Kollberg, *Fellow, IEEE*

Abstract— The conversion efficiency for planar $\text{Al}_{0.7}\text{GaAs}$ /GaAs heterostructure barrier varactor triplers is shown to be reduced from a theoretical efficiency of 10% to 3% due to self-heating. The reduction is in accordance with measurements on planar $\text{Al}_{0.7}\text{GaAs}$ /GaAs heterostructure barrier varactor (HBV) triplers to 261 GHz at room temperature and with low temperature tripler measurements to 255 GHz. The delivered maximum output power at 261 GHz is 2.0 mW. Future HBV designs should carefully consider and reduce the device thermal resistance and parasitic series resistance. Optimization of the RF circuit for a 10- μm diameter device yielded a delivered output power of 3.6 mW (2.5% conversion efficiency) at 234 GHz.

Index Terms— Heterostructure barrier varactor, self-heating, varactor frequency tripler.

I. INTRODUCTION

THE heterostructure barrier varactor (HBV) diode [1], [2] has received considerable attention as a promising symmetric varactor element for frequency multiplier applications at millimeter- and submillimeter-wave frequencies. Because of the symmetric capacitance–voltage (C – V) and the antisymmetric current–voltage (I – V) characteristics, only odd harmonics of an applied signal are produced, thus simplifying the design of a frequency tripler. By using several epitaxially stacked barriers, the power handling capability is increased due to distribution of power over several series devices, and a higher dynamic cutoff frequency for a given device area is achieved. However, to date the output power and efficiency from Schottky diode varactor multipliers are still somewhat superior to HBV multipliers [3]–[5].

In this paper we show that self-heating and parasitic series resistance are significant performance limiting factors for planar HBV's. The influence of series resistance and temperature on the tripler conversion efficiency is investigated in detail both theoretically and experimentally. With a novel temperature dependent HBV model, we are able to accurately

Manuscript received March 4, 1998; revised July 27, 1998. The review of this paper was arranged by Editor K. M. Lau. This work was also supported in part by grants from LM Ericsson and the Royal Swedish Academy of Sciences. The work of J. Stake was supported by the SSF High Speed Electronics program.

J. Stake, L. Dillner, and E. Kollberg are with the Microwave Electronics Laboratory, Chalmers University of Technology, SE-412 96 Göteborg, Sweden.

S. H. Jones and W. L. Bishop are with the University of Virginia, Charlottesville, VA 22903 USA.

C. Mann and J. Thornton are with the Rutherford Appleton Laboratory, Chilton, Oxon., U.K.

J. R. Jones is with Anadigics, Inc., Warren, NJ 07059 USA.

Publisher Item Identifier S 0018-9383(98)07835-6.

TABLE I
HBV LAYER STRUCTURE (UVA-NRL-1174)

Layer	Material	Doping [cm^{-3}]	Thickness [\AA]
13	InAs	5×10^{18}	100
12	$\text{In}_{1-x}\text{Ga}_x\text{As}$	5×10^{18}	400
11	GaAs	5×10^{18}	3000
10	GaAs	8×10^{16}	2500
9	GaAs	Undoped	35
8	$\text{Al}_{0.7}\text{GaAs}$	Undoped	200
7	GaAs	Undoped	35
6	GaAs	8×10^{16}	5000
5	GaAs	Undoped	35
4	$\text{Al}_{0.7}\text{GaAs}$	Undoped	200
3	GaAs	Undoped	35
2	GaAs	8×10^{16}	2500
1	GaAs	5×10^{18}	40000
0	GaAs	SI	-

reproduce experimental data and demonstrate the effects of device temperature and resistive loss. In addition, we report state-of-the-art results from tripler testing of a new batch planar four-barrier GaAs/ $\text{Al}_{0.7}\text{GaAs}$ HBV diodes (UVA-NRL-1174-17).

II. THE DEVICE

A. Fabrication

The $\text{Al}_{0.7}\text{GaAs}$ /GaAs epitaxial structure, MBE grown on SI GaAs substrate by the Naval Research Laboratory (NRL), consists of two barriers, and an n^{++} InAs/ $\text{In}_{1.0-0.0}\text{Ga}_{0.0-1.0}\text{As}$ /GaAs epitaxial capping layer to improve the specific contact resistance of the resulting ohmic contacts (see Table I). A back-to-back geometry, shown in Fig. 1, has been utilized to double the number of barriers and to compensate for asymmetries. The HBV's were fabricated using standard photolithography techniques for isolation and ohmic contact patterning, and reactive ion etching for anode definition and mesa/pad isolation [6]. The surface channel was planarized prior to airbridge formation using a low viscosity thermosetting epoxy and a planarizing superstrate [6], [7]. The fingers were Au-electroplated to a thickness of 2.5 μm and the finger width is 5 μm . Special attention is given to the ohmic contact formation and the anode isolation etch, since these steps affects the series resistance, and thus the tripler performance drastically (see Fig. 4). The Ni/Ge/Au ohmic metallic scheme was alloyed for 2 min at 375 $^{\circ}\text{C}$. The area of the anodes are 57 μm^2 and the separation between the two anodes is 5 μm .

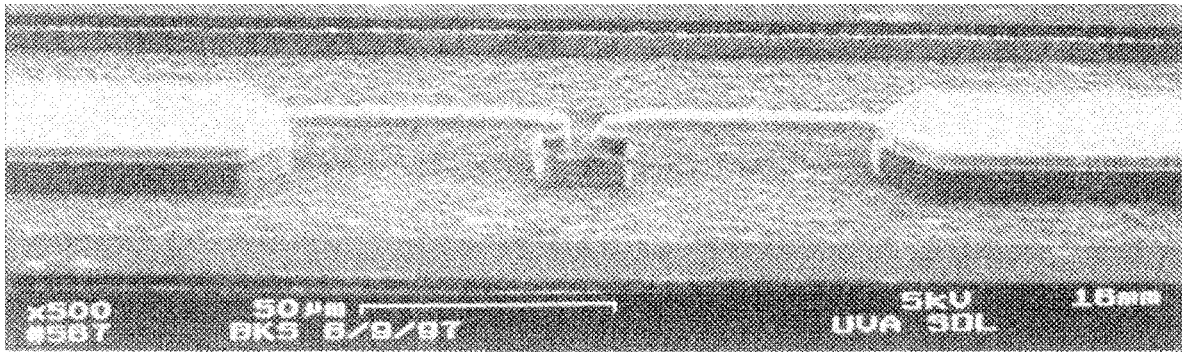


Fig. 1. Planar four-barrier GaAs/Al_{0.7}GaAs HBV chip (UVA-NRL-1174-17) before dicing and lapping.

B. C - V Model

In this work, we use a three-element quasi-static HBV model to predict and analyze the tripler performance: a series resistance, and a nonlinear current source in parallel to a nonlinear capacitor (see Fig. 3). The voltage across the nonlinear capacitor is expressed as a function of its charge as [8]

$$V(Q) = N \left(\frac{bQ}{\varepsilon_b A} + 2 \frac{sQ}{\varepsilon_d A} + \text{sign}(Q) \left(\frac{Q^2}{2qN_d \varepsilon_d A^2} + \frac{4kT}{q} \left(1 - e^{-(|Q|/2L_D A q N_d)} \right) \right) \right) \quad (1a)$$

$$L_D = \sqrt{\frac{kT \varepsilon_d}{q^2 N_d}} \quad (1b)$$

where

- N number of barriers;
- b barrier thickness,
- s undoped spacer layer thickness;
- A device area;
- N_d doping concentration in the modulation layer;
- $\varepsilon_b, \varepsilon_d$ dielectric constant in the barrier material and modulation layer respectively;
- T device temperature;
- q elementary charge;
- Q charge stored in the HBV.

The C - V characteristic can be calculated from the quasi-empirical expression (1) as dQ/dV and is shown together with the measured C - V curve in Fig. 2. The C - V characteristic was measured with an LCR-meter (HP4285) at 18 MHz.

C. Temperature Dependent I - V Model

To analyze the self-heating effect, a temperature dependent conduction current model was developed. The following empirical model describes the conduction current over the heterojunction barrier as a function of bias and temperature as

$$I(E_b) = A \cdot a \cdot T^2 \sinh \left(\frac{E_b}{E_o} \right) e^{-(\phi_b/kT)} \quad (2)$$

where E_b is the electric field in the barrier and can be implicitly calculated from (1) and Gauß's law, $Q = \varepsilon_b E_b$, or if electron

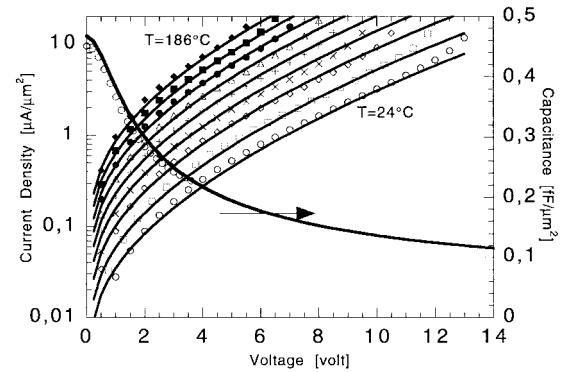


Fig. 2. Measured and modeled conduction current density and C - V characteristic for the 4-barrier HBV diode (UVA-NRL-1174). The C - V curve was measured at room temperature. The conduction current was measured on a hot-plate at different temperatures (RT-186°C). Due to symmetry, only positive voltages are shown in this figure.

screening effects are neglected as

$$E_b(V) = \text{sign}(V) \cdot qN_d \frac{b\varepsilon_d + 2s\varepsilon_b}{\varepsilon_b^2} \cdot \left(\sqrt{1 + \frac{2\varepsilon_d \varepsilon_d^2 |V|}{NqN_d(b\varepsilon_d + 2s\varepsilon_b)^2}} - 1 \right). \quad (3)$$

The parameters $a = 170 \text{ A}/(\text{m}^2\text{K}^2)$, $E_o = 4.2 \times 10^6 \text{ V}/\text{m}$, and $\phi_b = 0.17 \text{ eV}$ in (2) provide an excellent fit with measured I - V characteristic for the HBV's fabricated and operated at different temperatures (see Fig. 2).

D. Series Resistance and Thermal Resistance

The parasitic series resistance is the sum of the resistance of undepleted active layers, the spreading resistance, and the ohmic contact resistance. All these resistive elements have different temperature dependence. For simplicity, we assume the temperature dependence of the highly doped buffer layer (spreading resistance) and the modulation layers to be the same as for intrinsic GaAs material ($\propto T^{1.0}$) [9] and the contact resistance is assumed to be temperature independent. In general, it is difficult to determine the series resistance of HBV's or back-to-back Schottky varactor diodes from DC-measurements given the large junction resistance over the normal operating range of the device. Therefore, we have chosen a simple approach to model the temperature dependence of the series resistance. For

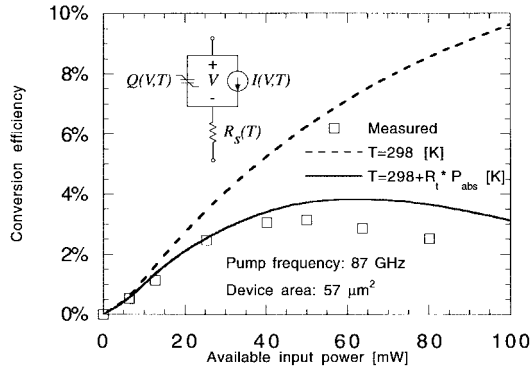


Fig. 3. Measured and simulated tripler conversion efficiency versus available power for the HBV tripler with a 8 μm diameter device (UVA-NRL-1174-17) at a fundamental frequency of 87 GHz. The measurements were performed at room temperature. For the simulations, an input loss of 1 dB and an output loss of 2 dB in the waveguide circuit were assumed.

the HBV described and with a specific contact resistance of $\sim 10^{-6} \cdot \text{cm}^2$, a room temperature parasitic series resistance of 16Ω was estimated; this value was calculated using standard expressions for contact resistance, mesa resistance, spreading resistance in the n^{++} island that connects the two diodes, and using impurity dependent mobility values for GaAs [9]. For simplicity, we approximate the parasitic series resistance within the operated temperature range as

$$R_s(T) = \underbrace{\frac{200}{A}}_{2r_c/A} + \left(\underbrace{4 + \frac{20}{\sqrt{A}}}_{\text{Spreading Resistance}} + \underbrace{\frac{320}{A}}_{\text{Intrinsic Resistance}} \right) \frac{T}{298} \quad [\Omega] \quad (4)$$

where A is the anode area in μm^2 . The first term is the contact resistance and the second accounts for the finite semiconductor conductivity: spreading resistance in the n^{++} island and the intrinsic active layers.

Furthermore, assuming a point heat-source in the middle of the active region, Jones [10] has estimated the thermal resistance through the finger and the GaAs substrate to $R_t \approx 2 \text{ K/mW}$ for this device geometry using a combination of analytical models and FEM-simulations. We have therefore used this value for the thermal resistance and assumed a reverse proportional dependency on the anode diameter in our analytical model as

$$R_t = \frac{15}{\sqrt{A}} \quad [\text{K/mW}]. \quad (5)$$

The main contribution to the thermal resistance is through the n^{++} buffer-region and the substrate to the pad-area (Fig. 1). Consequently, the active region temperature can be as high as $125 \text{ }^\circ\text{C}$ for an absorbed input power of 50 mW.

E. RF Performance Modeling for Efficiency and Output Power

The actual RF performance of the device is calculated using the equivalent circuit model for HBV's described above and shown in Figs. 3 and 4. Using (1)–(5), the equivalent circuit

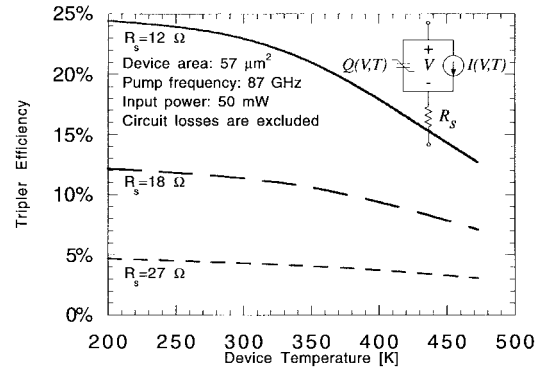


Fig. 4. Simulated maximum conversion efficiency ($\times 3$) versus device (junction) temperature for the HBV tripler with an 8- μm diameter device (UVA-NRL-1174-17) at a fundamental frequency of 87 GHz. The absorbed input power is 50 mW and circuit losses are excluded.

model shown in Fig. 3, and an in-house harmonic-balance (HB) routine [11], the HBV output power and efficiency can be directly calculated for input power and parasitic series resistance. The HB-code uses a splitting method [12] to solve the harmonic balance equation for the linear embedding network and the nonlinear diode, and has been verified against commercial microwave simulation tools such as the HP-MDS program. The effect of current saturation [13] is not included in the above HBV-model. However, since the peak value of the current waveform ($< 90 \text{ mA}$) was less than the saturation current in the undepleted layers during all simulations, the above quasi-static HBV-model is accurate enough for our purpose. The saturation current is estimated to be 130 mA ($= AqN_d v_{\text{max}}$) for an 8- μm diode and assuming a maximum electron velocity of $1.8 \times 10^5 \text{ m/s}$ [14]. The HB analysis is used to illuminate the decrease in HBV performance as the input power (device temperature) is increased to typical values.

III. MEASUREMENTS

The tripler block used was a Rutherford Appleton Laboratory (RAL) block (NB6) and was originally designed for use with whisker contacted Schottky varactor diodes. The planar HBV chip, lapped to a thickness of $50 \mu\text{m}$, was mounted across the output waveguide. The waveguide block is equipped with a single backshort tuner at the output and both backshort and E-plane tuner at the input.

A. Room Temperature Experimental Setup

Input power was provided by a Thompson CSF Carcinotron which could be electronically tuned over a frequency range from 75 to 100 GHz. Sufficient power was available that an isolator, wavemeter, attenuator and directional couplers could be included in the input chain to determine input and reflected power levels along with frequency. Both input and output powers were measured using separate Anritsu power heads and meter type ML 83A, which had previously been compared with a Thomas Keating power meter and had been found to agree to $\pm 5\%$. In order to mate the output waveguide to that of the output power head it was necessary to include a waveguide

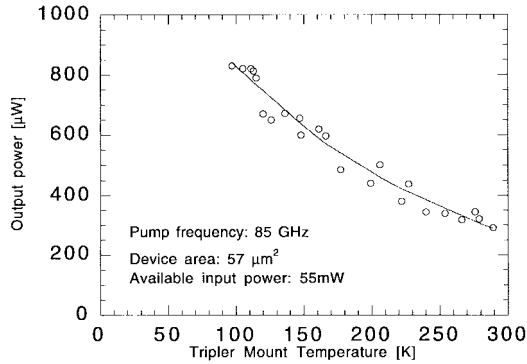


Fig. 5. Measured output power at a fundamental of 85 GHz obtained for an 8- μm diameter device (UVA-NRL-1174-17) versus tripler mount temperature. The available input power is ~ 55 mW.

transformer section, the additional loss this introduced was not corrected for.

A Fourier transform spectrometer was later used to ensure that there was no parasitic generator of even-order harmonics from the HBV tripler.

B. Cooled Temperature Experimental Setup

The tripler mount (RAL-DB2a) with a 57- μm^2 area device was mounted into a vacuum chamber and the input power was provided through a WR-10 waveguide, vacuum window and a J. E. Carlstrom (H270) Gunn oscillator (114 mW@85 GHz). Output power was extracted through a horn antenna, a mylar window, and finally measured outside the chamber with a Thomas Keating power meter. To thermally isolate the tripler mount from the environment, a piece of stainless steel waveguide was used in the input circuit. The measured available input power into the tripler block at 85 GHz was ~ 55 mW. The input tuners and the output tuner were optimized at room temperature for maximum tripler efficiency. After evacuating the chamber and during cooling, the only tuning-possibility of the tripler was through changing the pump frequency.

IV. RESULTS AND DISCUSSION

For an input power of 50 mW, the maximum output power was obtained at a pump frequency of 87 GHz. The HBV was DC-short circuited during RF testing. A maximum output power of greater than 2 mW was generated at 261 GHz with an available power of 80 mW, as shown in Fig. 3. A peak flange-to-flange efficiency of 3.1% was achieved. During the whole test-series, the return loss was tuned to better than 15 dB. The estimated losses at the input and output circuit are approximately 1 and 2 dB, respectively. Although these are the best planar HBV results in terms of output power in the output frequency range 150–300 GHz reported to date [15], [16], they are still below the predicted and anticipated results as described below.

The predicted conversion efficiency (for the HBV described above) at 25 °C and a series resistance of 16 Ω , is as high as $\sim 10\%$ for input power of about 100 mW, as shown in Fig. 3 by the dotted line. The discrepancy between theory and

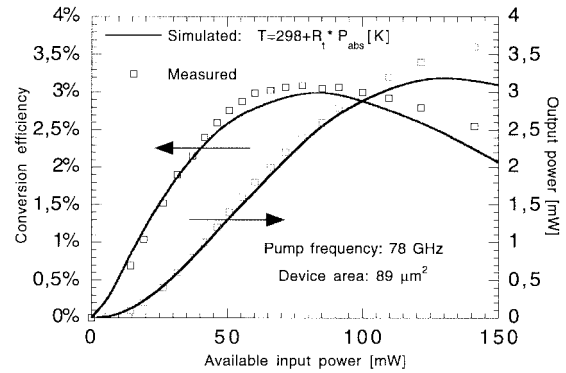


Fig. 6. Measured and simulated output power and efficiency for an output frequency of 234 GHz obtained for a 10- μm diameter device (UVA-NRL-1174-17). For the simulations, an input loss of 1 dB and an output loss of 2 dB in the waveguide circuit were assumed.

experiment can be explained by self-heating as the input power increases. The solid line in Fig. 3 demonstrates the effects of self-heating when a thermal resistance of 2 K/mW is used in the HB simulations. Due to self-heating, the efficiency reaches a maximum of about 3% at a pump power of 50 mW. With the temperature dependent HBV model, described in Section II, and if we assume the device temperature to increase linearly with absorbed input power, it was possible to reproduce the measured tripler efficiency versus available pump power (see boxes and solid line in Fig. 3). A linear assumption between temperature and absorbed power is reasonable since the conversion efficiency is small. For each temperature and input power, the impedances at the fundamental and the third harmonic were optimized for maximum conversion efficiency. Furthermore, current harmonics higher than the output frequency were kept at zero for simulation purposes.

The theoretical influence of device temperature and parasitic series resistance, R_s , on maximum conversion efficiency for the planar HBV tripler is shown in Fig. 4. The input power was kept constant at 50 mW and circuit losses were excluded. At elevated temperatures, the efficiency degrades due to an increased conduction (leakage) current [see (2) and Fig. 2] and a reduced $C_{\text{max}}/C_{\text{min}}$ ratio (1). To experimentally verify the effect of high conduction current due to self-heating and its negative affect on the tripler efficiency, the tripler block was cooled while measuring the output power for a constant available input power of ~ 55 mW. When the diode is cooled, the leakage current becomes negligible and the efficiency increases with $\sim 300\%$ (4.7 dB), as shown in Fig. 5. The reason for a lower absolute third harmonic power compared to the room temperature experiment is due to larger losses at the output (Section III-B). Similar experiments with GaAs Schottky varactor doublers at 160 GHz resulted in an overall improvement of $\sim 25\%$ (1 dB) [17]. Consequently, the strong temperature dependence of low barrier height HBV's is mainly due to a reduced conduction current rather than the effect of improved electron mobility and lower circuit losses. Finally, the strong effect of the parasitic series resistance is shown in Fig. 4.

In an attempt to determine the maximum power that could be obtained from the HBV diodes a second tripler waveguide

block, RAL DB2a was used. The RF embedding circuit in this tripler block which can be readily modified and was therefore empirically optimized for the 10-m diameter HBV diodes, anode area $89 \mu\text{m}^2$. This diode was chosen, as its larger area should enable it to handle more input power and thus provide more output power. While the diode anodes are larger the same chip architecture has been used, the parasitic electrical (4) and thermal resistance (5) is therefore essentially the same as that found for the smaller area devices. No overall improvement in the measured efficiency was therefore expected nor gained, however, the maximum available output power was increased to 3.6 mW. A plot of the experimental results for an output frequency of 234 GHz together with HB simulations are shown in Fig. 6.

V. CONCLUSIONS

Current planar HBV diodes suffer from a high conduction current due to a low effective electron barrier and a high thermal resistance. If the effective barrier height is increased, e.g., with a thin layer of AlAs in the middle of the barrier [18]–[20] or the use of InGaAs spacer layers, the conduction current will be drastically reduced and hence the conversion efficiency of a HBV multiplier is expected to be less sensitive to heating. However, the efficiency depends critically on the parasitic series resistance which generally increases with the temperature. Furthermore, the effect of current saturation is increased with temperature due to a lower maximum electron velocity at elevated temperatures [14], [17]. Therefore, special attention should be paid to heat transfer properties of the multiplier mount and the chip architecture itself during the circuit and diode design process.

ACKNOWLEDGMENT

The authors thank A. Lichtenberger, B. Sarpong, S. Marazita, and T. Crove of the Semiconductor Device Laboratory, University of Virginia, for their support during device fabrication.

REFERENCES

- [1] E. L. Kollberg and A. Rydberg, "Quantum-barrier-varactor diode for high efficiency millimeter-wave multipliers," *Electron. Lett.*, vol. 25, pp. 1696–1697, 1989.
- [2] A. Rydberg, H. Grönqvist, and E. L. Kollberg, "Millimeter- and submillimeter-wave multipliers using quantum-barrier-varactor (QBV) diodes," *IEEE Trans. Electron Devices*, vol. 11, pp. 373–375, 1990.
- [3] N. R. Erickson, "High efficiency submillimeter frequency multipliers," presented at IEEE MTT-S, Dallas, TX, 1990, pp. 1301–1304.
- [4] ———, "A high efficiency frequency tripler for 230 GHz," presented at 12th European Microwave Conf, Helsinki, Finland, 1982, pp. 288–292.
- [5] J. Thornton, C. M. Mann, and P. D. Maagt, "A high power 270 GHz frequency tripler featuring a Schottky diode parallel pair," presented at IEEE-MTT Int. Microwave Symp. Digest, Denver, CO, 1997, pp. 957–958.
- [6] J. R. Jones, W. L. Bishop, S. H. Jones, and G. B. Tait, "Planar multibarrier 80/240 GHz heterostructure barrier varactor triplers," *IEEE Trans. Microwave Theory Tech.*, vol. 45, pp. 512–518, 1997.
- [7] W. L. Bishop, K. McKinney, R. J. Mattauch, T. W. Crowe, and G. Green, "A novel whiskerless Schottky diode for millimeter and submillimeter wave applications," presented at 1987 IEEE MTT-S Int. Microwave Symp., Las Vegas, NV, 1987, pp. 607–610.

- [8] L. Dillner, J. Stake, and E. L. Kollberg, "Modeling of the heterostructure barrier varactor diode," presented at 1997 International Semiconductor Device Research Symp., Charlottesville, VA, 1997, pp. 179–182.
- [9] S. M. Sze, "Carrier transport phenomena: Mobility," in *Physics of Semiconductor Devices*, 2nd ed. Singapore: Wiley, 1981, pp. 27–38.
- [10] J. R. Jones, S. H. Jones, and G. B. Tait, "Self-consistent physics-based numerical device/harmonic-balance circuit analysis of heterostructure barrier varactors including thermal effects," presented at *Sixth Int. Symp. Space Terahertz Technology*, Pasadena, CA, 1995, pp. 423–441.
- [11] L. Dillner and J. Stake, "Analysis of heterostructure barrier varactor frequency multipliers," Tech. Rep. 27, Dept. Microwave Technol. Chalmers Univ. Technology, Göteborg, Sweden, Nov. 1996.
- [12] S. A. Maas, *Nonlinear Microwave Circuits*. Boston, MA: Artech House, 1988.
- [13] E. L. Kollberg, T. J. Tolmunen, M. A. Frerking, and J. R. East, "Current saturation in submillimeter wave varactors," *IEEE Trans. Microwave Theory Tech.*, vol. 40, pp. 831–838, 1992.
- [14] J. G. Ruch and W. Fawcett, "Temperature dependence of the transport properties of gallium arsenide determined by a Monte Carlo method," *J. Appl. Phys.*, vol. 41, pp. 3843–3849, 1970.
- [15] D. Choudhury, M. A. Frerking, and P. D. Batelaan, "A 200-GHz tripler using a single barrier varactor," *IEEE Trans. Microwave Theory Tech.*, vol. 41, pp. 595–599, 1993.
- [16] T. J. Tolmunen, A. V. Räisänen, E. Brown, H. Grönqvist, and S. M. Nilsen, "Experiments with single barrier varactor tripler and quintupler at millimeter wavelengths," presented at Fifth Int. Symp. Space Terahertz Technology, 1994, pp. 486–496.
- [17] J. T. Louhi, A. V. Räisänen, and N. R. Erickson, "Cooled Schottky varactor frequency multipliers at submillimeter wavelengths," *IEEE Trans. Microwave Theory Tech.*, vol. 41, pp. 565–571, 1993.
- [18] K. Krishnamurthi, S. M. Nilsen, and R. G. Harrison, "GaAs single-barrier varactors for millimeter-wave triplers: Guidelines for enhanced performance," *IEEE Trans. Microwave Theory Tech.*, vol. 42, pp. 2512–2516, 1994.
- [19] Y. Fu, J. Stake, L. Dillner, M. Willander, and E. L. Kollberg, "Al-GaAs/GaAs and InAlAs/InGaAs heterostructure barrier varactors," *J. Appl. Phys.*, vol. 82, pp. 5568–5572, 1997.
- [20] E. Lheurette, P. Mounaix, P. Salzenstein, F. Mollot, and D. Lippens, "High performance InP-based heterostructure barrier varactors in single and stack configuration," *Electron. Lett.*, vol. 32, pp. 1417–1418, 1996.



Jan Stake (M'98) was born in Uddevalla, Sweden, in 1971. He received the Civingenjör (M.Sc.) degree in electrical engineering and the Tekn. Lic. degree in microwave electronics from Chalmers University of Technology, Göteborg, Sweden, in 1994 and 1996, respectively. He is currently pursuing the Ph.D. degree at Chalmers University of Technology. As part of his Ph.D. studies, he spent four months in 1997 at the University of Virginia, Charlottesville.

His interests are devices for millimeter-wave applications and device fabrication technologies.



Lars Dillner was born in Säffle, Sweden, in 1968. He received the M.S. degree in engineering physics and the Tekn. Lic. degree in microwave electronics in Chalmers University of Technology, Göteborg, Sweden, in 1994 and 1998, respectively. He is currently pursuing the Ph.D. degree at the Microwave Electronics Laboratory, Chalmers University of Technology.

His interests are varactor diodes and frequency multipliers.

Stephen H. Jones (S'85–M'89), for a biography, see p. 1882 of the September 1998 issue of this TRANSACTIONS.



Chris M. Mann was born in London, U.K., in 1962. He received the B.Sc. degree (honors) from Coventry Polytechnic, Lanchester, U.K., in 1985, and the Ph.D. degree from the University of London, London, U.K., in 1992.

From 1985 to 1992, he was an Associate Researcher at the Rutherford Appleton Laboratory (RAL), Oxon., U.K., where he worked on numerous aspects of millimeter-wave technology, including superconductor/insulator/superconductor (SIS) junction fabrication, space hardware, and a novel 183-GHz subharmonic mixer. In 1992, he joined the Photodynamics Research Center, Sendai, Japan, where he was involved with the design of corner cube mixers at 1.4 THz and the use of analytical models for the prediction of waveguide-circuit embedding impedance. In 1994, he returned to RAL, playing a leading role in the design, fabrication, and testing of the world's first 2.5 THz waveguide mixer in 1995. He has since continued this work, and is also working on the optimization of submillimeter-wave frequency multipliers and subharmonic mixers and is currently pioneering waveguide micromachining techniques in order to realize completely integrated submillimeter-wave RF frontends.



John Thornton was born in Lancastershire, U.K., in 1968. He received the B.Sc. degree in physics from the University of York, York, U.K., in 1989, and the M.Sc. degree from the University of Portsmouth, Portsmouth, U.K., in 1995.

From 1995 to 1997, he worked with the Millimeter Wave Technology Group, Rutherford Appleton Laboratory (RAL), Oxon., U.K., where he specialized in the development of solid-state frequency multipliers for spaceborne receivers from 200 to 500 GHz. He is currently with the Department of

Engineering Science, University of Oxford, U.K., where his recent research has involved the development of novel modulated microwave reflectors, which operate as passive transponders at commercial radar frequencies, a technique pioneered at Oxford.



J. Robert Jones (M'95) was born in Trenton, NJ, in 1968. He received the B.S., M.S., and Ph.D. degrees in electrical engineering from the University of Virginia, Charlottesville, in 1990, 1992, and 1996, respectively.

From 1989 to 1995, he was a Research Assistant in the Semiconductor Device Laboratory, University of Virginia, where his research interests included semiconductor heterostructure device physics and modeling, nonlinear microwave and millimeter-wave circuit analysis and design, and solid-state device fabrication. In December 1995, he joined the Technical Staff, Anadigics, Inc., Warren, NJ, as a Senior Device Engineer. Since September 1997, he has served as Manager of the Device Modeling and Simulation Group, Anadigics, Inc., where he is responsible for the characterization and compact modeling of active and passive components and the physical simulation of ion-implanted and epitaxial devices, including MESFET's and HEMT's.

Dr. Jones is a member of Tau Beta Pi, Eta Kappa Nu, and Sigma Xi.



William L. Bishop (S'88-M'93) is a received the B.S. degree in engineering science from the University of Virginia, Charlottesville, in 1969.

He is currently a Research Scientist in the Semiconductor Laboratory, University of Virginia. For the past 15 years, he has been actively involved in the design and fabrication of millimeter and submillimeter wavelength Schottky diodes. His primary interest is the development of new technology for the fabrication of whisker-contacted and planar diodes, which improves performance, reliability,

and yield. He is a founder and Vice President of Virginia Diodes, Inc.

Mr. Bishop is a member of Sigma Xi.



Erik Kollberg (M'83-SM'83-F'90) has been a Professor in the School of Electrical and Computer Engineering, Chalmers University of Technology, Göteborg, Sweden, since 1980. He was Acting Dean of Electrical and Computer Engineering from 1987 to 1990. From 1983 to 1976, he was with Onsala Space Observatory, researching low-noise maser amplifiers used for radio astronomy observations. His research has since comprised low-noise millimeter-wave Schottky diode mixers, varactor diode multipliers, superconducting quasi-

particle mixers, quantum well devices, submillimeter-wave hot electron mixers and three terminal devices, such as FET's and HBT's. He has published about 180 papers on the above subjects. He is the inventor of the heterostructure barrier varactor diode. He has been a Visiting Guest Professor at Ecole Normal Supérieure, Paris, France, in the summers of 1983, 1984, and 1987, and was a Distinguished Fairchild Scholar at the California Institute of Technology, Pasadena, in 1989.

Dr. Kollberg received the 1982 Microwave Prize from the 12th European Microwave Conference, Helsinki, Finland, the Gustaf Dahlén Gold Medal in 1986, and was elected IEEE Fellow in 1990. He is a member of the Royal Swedish Academy of Science and the Royal Swedish Academy of Engineering Sciences.